Noncovalent Functionalization of BN Nanotubes with Perylene Derivative Molecules: An *ab Initio* Study

Gaoyang Gou,[†] Bicai Pan,[†,‡,*] and Lei Shi[†,*]

[†]Hefei National Laboratory for Physical Science at Microscale and [‡]Department of Physics, University of Science and Technology of China, Hefei 230026, P. R. China

ABSTRACT The noncovalent functionalization of boron nitride nanotubes (BNNTs) with perylene-derived molecules has been reported experimentally [Wang *et al. J. Am. Chem. Soc.* 2008, *130*, 8144]. Here we study the structural and electronic properties for the perylene-derivative functionalized BNNTs using first-principles calculations. Our calculations highlight the electronic structure modifications of BNNT through the noncovalent functionalization and demonstrate that van der Waals interactions between the adsorbed perylene derivatives and host BN layers facilitate the functionalization. We also provide an explanation for the red-shift of optical adsorption bands observed in experiment and discuss improvements in theoretical calculations of noncovalently functionalized BNNTs.

KEYWORDS: boron nitride nanotubes · *ab initio* calculations · noncovalent functionalization · electronic structures · absorption spectra

Since the discovery of carbon nanotubes (CNTs), extensive studies have been performed on analogous tubular nanomaterials, such as boron nitride nanotubes (BNNTs).[1,2] In contrast with metallic or semiconducting CNTs, BNNTs are wide-gap semiconductors, whose band gaps (~5.5 eV) are almost independent of tube structure.[3] In addition, although they have comparable thermal conductivities[5] and mechanical properties,[6,7] BNNTs exhibit better chemical stability and resistance to oxidation over CNTs.[4] These advantageous properties make BNNTs promising materials for applications in nanoscale electronics and nanocomposite devices.

Chemical functionalization is a commonly used method to enrich the physical properties of nanotubes. Especially, chemical functionalization of BNNT has become a subject of extensive studies.[8] It is reported that covalent functionalizations using adatoms, organic molecules, and functional groups can effectively change the electronic structures,[9,10] magnetic properties,[11,12] and solubilities[13,14] of BNNTs. Noncovalent functionalizations of BNNTs, which are mediated by weak interactions rather than covalent bonds, have also been extensively explored. For example, the noncovalent functionalization of BNNTs with the conjugated polymer PmPV has been achieved experimentally.[15] These PmPV-functionalized BNNTs are soluble in various organic solvents but insoluble in water. On the basis of this finding, polymer wrapping technology has been developed to purify the BNNT samples.[15] It is noted that not every organic molecule can be used for BNNTs functionalization. Researchers have spent great efforts searching for reagents suitable for noncovalent functionalization of BNNTs.

Very recently, Wang *et al.*[16] reported the noncovalent functionalization of BNNTs in aqueous solution through π-stacking of an anionic perylene derivative, namely PTAS. The functionalized nanotubes are soluble in aqueous solution. Moreover, in UV−visible absorption spectra, a significant redshift of the optical bands were observed for PTAS-functionalized BNNTs, relative to pristine PTAS. The authors attribute the redshift to the strong π−π interactions as well as efficient electron transfer between the molecules and nanotubes. Although Wang *et al.* presents a pioneering experimental work on the noncovalent functionalization of BNNTs, some issues are still unresolved. For example, the easy grafting of BNNTs by PTAS was found experimentally, but what is the nature of the interaction between the two? Especially, the physical origins for the shift of optical bands, which were also observed in other noncovalently functionalized BNNT systems,[15,17,18] remain unclear. These questions merit further theoretical investigation.

*Address correspondence to bcpan@ustc.edu.cn, shil@ustc.edu.cn.

Received for review July 27, 2009 and accepted February 05, 2010.

Published online February 15, 2010. 10.1021/nn900872t

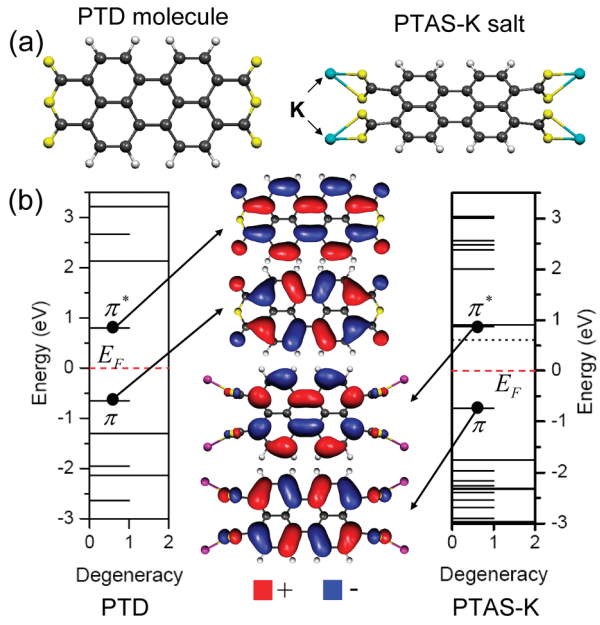

Figure 1. (a) Atomic structures of PTD and PTAS−K molecules. C, H, O, and K atoms are represented by black, white, yellow, and cyan balls respectively. (b) Energetic level diagrams and isosurface of charge density for π and π^* bands in the respective molecules. The pseudostate of PTAS−K is indicated by a black dashed line. The isosurface value is ±0.05 eV/Å^3 (distinguished by red and blue surfaces). The Fermi energy levels are set at energy zero, indicated by red dashed lines.

In this study, we model the experimental findings of Wang *et al.* with first-principles calculations, and investigate the structural and electronic properties of perylene-derivative functionalized BNNTs. On the basis of our calculations, we conclude that the perylene derivatives are attached to BN layers by van der Waals interactions, which could lead to the effective noncovalent functionalization of BNNTs. Our study also explains the redshift of the optical adsorption spectra observed in experiment.

RESULTS AND DISCUSSIONS

Isolated Perylene Derivative Molecules. Experimentally, the perylene derivative molecules were dissolved in the aqueous solution, namely PTAS solution. The PTAS-functionalized BNNTs (denoted as PTAS−BNNTs) were also prepared in this solution. To simulate the experimental results, we should provide the theoretical understanding to the electronic and optical properties of PTAS solution at first.

The PTAS solution was prepared by the alkaline hydrolysis of PTD molecules (the experimental details can be found in ref 16). Because the hydrolytic reaction is reversible, both reactant PTD and hydrolytic product PTAS molecules should coexist in the aqueous PTAS solution. To simulate the experimental PTAS solution, both molecules should then be taken into consideration.

PTD and PTAS are perylene derivative molecules, both of which are composed of the alternating benzene rings, but they carry different functional groups. Typically, PTD carries acid anhydride groups, whereas PTAS has four carboxylate groups at the both sides. As opposed to the neutral PTD molecules, PTAS molecules are actually negatively charged anions in the aqueous solution. Therefore, we employ a neutral molecule (PTD in Figure 1a) to represent PTD molecules; for the anionic PTAS, the carboxylic acid potassium salt (namely PTAS−K in Figure 1a) is taken as an alternative. The anionic PTAS and PTAS−K are isovalent (equal number of valence electrons) and almost share the same bonding configuration. We therefore expect that PTAS−K is an appropriate representation for experimental PTAS anions.

The electronic structures and isosurface of charge densities for PTD and PTAS−K molecules are given in Figure 1b. Both of the molecules are π-electron systems, with π states as their HOMOs and π^* states as LUMOs. In PTAS−K, there also exists a degenerate state (indicated by dashed line) between Fermi energy level and its π^* band. Such a state corresponds to the empty orbitals of K atoms. Since K atoms are completely ionized in the anionic PTAS, this degenerate state is only a pseudostate involved in our simulations, one that does not exist under the experimental conditions. Using LDA functional, the band gap ($\pi-\pi^*$ gap) values of PTD and PTAS−K are calculated to be 1.45 and 1.61 eV, respectively.

From electronic point of view, both PTD and PTAS−K are π-conjugated molecules. As displayed in Figure 1b, both π and π^* states of the two molecules are composed of the p_z atomic orbitals from C atoms, which exhibit the Hückel-like delocalized characters. Compared to PTD, the carboxylate groups in PTAS−K can provide extra delocalized π electrons (Π_3^4), leading to a larger $\pi-\pi^*$ gap in PTAS−K.

To understand the experimental UV−visible adsorption spectra for PTAS, the optical adsorption spectra are simulated in our work. The computational details of this part of the calculations can be found elsewhere.[19] Figure 2a shows our simulated optical adsorption spectra for isolated PTD and PTAS−K. The main optical peak for a π-conjugated system, such as PTD and PTAS−K, should originate from the electronic interband transitions between π and π^* bands. Compared to experimental spectra, our simulated optical peaks are lower in energy. This discrepancy comes from the underestimation of the band gaps in LDA or GGA calculations.[20,21] However, in this study we mainly focus on the relative change of the band gap, we can therefore expect that the band gap error is largely canceled when comparing different systems.

In our simulations, the main profiles for the combined spectrum, which is the superposition of optical peaks for the isolated PTD and PTAS−K, can well match the experimental UV−visible adsorption spectrum for PTAS aqueous solution (Figure 2). We also find that the

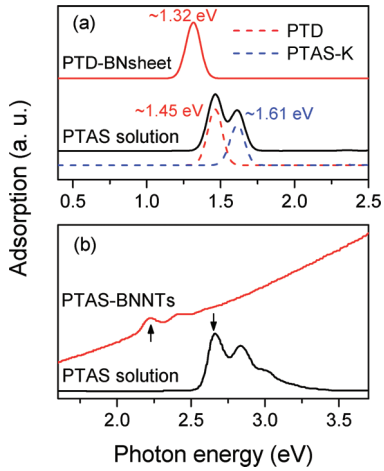

Figure 2. (a) Our calculated optical adsorption spectra for isolated PTD, PTAS−K, and PTD−BNsheet. (b) The experimental UV−visible adsorption spectra of PTAS−BNNTs and PTAS aqueous solution. The optical peaks corresponding to the fingerprint of PTD are indicated by arrows. Note: different energy scales are in used in panels a and b.

pseudostate in PTAS−K has no contribution to the optical response of the system, indicating that such a pseudostate can be neglected. Compared to our simulated spectra, the two main optical peaks experimentally observed can be identified as the fingerprints for PTD and PTAS−K (anionic PTAS), respectively. In particular, our calculated energy difference between optical peaks of PTD and PTAS−K is 0.16 eV, coming quite close to the experimental value of 0.17 eV.

Adsorption of the Perylene Derivative Molecules on BN Tubes. In this section, we start our analysis by briefly reviewing some experimental details for preparation of PTAS-functionalized BNNTs. In experiments, the diameter of BNNTs synthesized using CVD method is on the order of tens of nanometers.[16] Moreover, the thermogravimetric analysis (TGA) results show that the amount of the perylene derivative molecules attached on BNNTs is very small, indicating the attached molecules are isolated. In this context, the PTAS−BN tube system can be well modeled using the supercell approach. Owing to the fact that the diameters of BNNTs are really large, with negligible curvature effect, we employ a planar BN sheet as the prototype for the experimental large-size BN tube.

To understand the interaction between perylene derivative molecules and BNNTs, the adsorption of PTD and PTAS−K on BN sheet should be simulated. As it is discussed above, both PTD and PTAS−K are π-conjugated molecules, having similar structural and electronic properties. Experimentally, it has also been observed that two optical peaks corresponding to the fingerprints of PTD and PTAS−K (anionic PTAS) were almost shifted equally in energy. The above findings may indicate that PTD and PTAS−K share the same nature of interaction with BN nanotubes. Therefore, in the following discussion, the PTD-functionalized BN

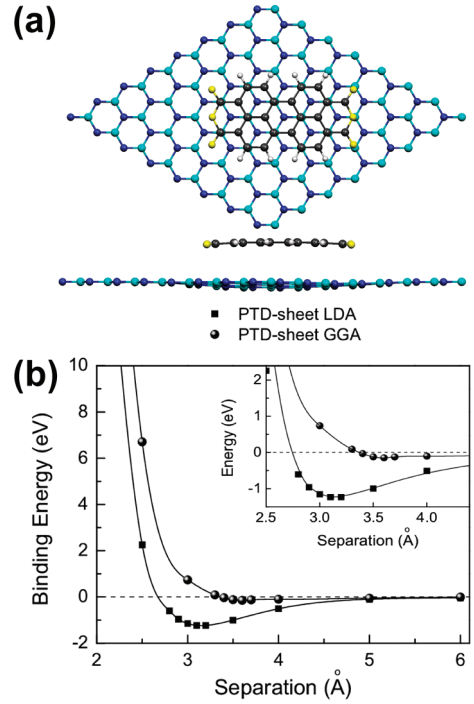

Figure 3. (a) Atomic structures (top and side views) and (b) binding energy curves for the adsorption of a PTD molecule on a BN sheet. The binding energies are calculated using LDA (squares) and GGA functionals (circles), respectively. Inset: A close view to the binding energy minimum. Light-blue (dark-blue) balls represent B(N) atoms.

sheet (denoted as PTD−BNsheet) is taken as a representative example for a detailed analysis.

For the adsorption of a planar PTD molecule on the BN sheet, we find that the most stable adsorption configuration is a structure where the center of benzene ring in PTD molecule is placed right on the top of a B(N) atom in the BN sheet (See Figure 3a). Such a stacking configuration is structurally similar to other π-stacking systems, such as bilayer graphene nanonribbons.[22]

To evaluate the interaction within molecule−sheet system, we simulate the binding energy for the adsorption of PTD molecule on BN sheet. For the noncovalent functionalization system, usually two subsystem (such as PTD and BN sheet) interact with each other through the van der Waals interactions. Because of the nonlocal nature of the van der Waals interaction, such an interaction cannot be precisely described by either LDA or GGA functional.[23] Therefore the interaction between PTD and BN sheet should be computed with particular care. In our calculation, the localized atomic-like orbital is employed as the basis set. When calculating the interaction between PTD molecule and BN sheet, the basis between isolated molecule, sheet, and the complete PTD−BNsheet system are not the same: the basis for the complete PTD-sheet system is usually larger, which can lead to an unphysical energy lowering of the system, and therefore gives a wrong binding energy.[24] In our calculation, this kind of basis set superposition error (BSSE) has been corrected using the

counterpoise method,[25] as the correct binding energy is given by the following relation:

$$E_{binding} = E(\text{BNsheet} + \text{PTD}) - [E(\text{BNsheet} + \text{PTD}_{ghost}) + E(\text{BNsheet}_{ghost} + \text{PTD})] \quad (1)$$

The "ghost" subsystems correspond to the additional localized basis centered at the atomic position of the PTD or BN sheet, but without any atomic potential. By including these "ghost" subsystems, the correct binding energy is defined as the DFT total energy difference between the complete system and the two subsystems.

To calculate the binding energy between PTD and BN sheet, we perform the constrained geometry relaxation by fixing the spacing between PTD and BN sheet, while their planar coordinates are fully relaxed. Figure 3b displays the calculated binding energy for PTD−BNsheet as a function of the molecule−sheet separation, with the adsorption configuration shown in Figure 3a.

The binding energy curves obtained from LDA and GGA functional calculations are completely different: LDA predicts a binding ground state between PTD and BNsheet, with the equilibrium distance of 3.15 Å and binding energy of −1.23 eV. Its binding energy curve exhibits the Lennard-Jones like characters, and equilibrium distance is within the bond length range of typical van der Waals bond, indicating PTD molecule adsorbs on BN sheet mainly through the van der Waals interactions. However, within GGA calculations, there is almost no effective binding between PTD and BN sheet.

Our findings on the PTD−BNsheet are similar to other van der Waals adsorption systems. For instance, the geometry of graphite is correctly described by LDA calculations, only its interlayer binding energy is underestimated by 50%. Whereas GGA calculations fail to predict the binding ground state for graphite at all.[26] Compared to GGA functional, LDA can be used as a reasonable approximation for the van der Waals interaction systems through fortuitous cancelations of errors between exchange and correlation energy.[27,28] In light of this finding, we expect that LDA calculations are able to predict the physical properties of PTD−BNsheet system qualitatively right. Therefore in our work, by using LDA calculations, we mainly focus on the binding trend between PTD and BN system, rather than the accurate values for their interaction energy.

In the next step, we preform the fully structural relaxations for PTD−BNsheet system without geometrical constraint. In the optimized structure, the planar molecule and BN sheet display a structural buckling, with the atoms around the adsorption area moving slightly outward from the molecule or sheet surface (Figure 3a). Moreover, the binding energy of the system further goes down (−1.47 eV by LDA calculations). The structural buckling and the large magnitude of the

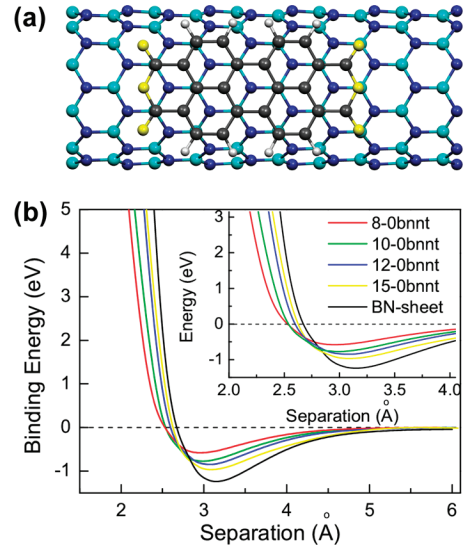

Figure 4. (a) Atomic structure (top view) for adsorption of a PTD molecule on a (10, 0) BNNT. (b) The simulated binding energy curves for the adsorption of a PTD molecule on BNNTS with different radii and a BN sheet. The binding energies are calculated using LDA functionals. Inset: a close view to the binding energy minimum.

binding energy within the molecule−sheet system indicates that the interaction between PTD and BN sheet is extraordinarily strong. Such a finding can provide a natural explanation to the experimental result that the perylene derivative molecules can be easily attached on BNNTs.

In the above discussions, we employ a planar BN-sheet to represent the experimental BNNT samples, neglecting the curvature effect. But under the real experimental environment, due to the presence of the small-radius tubes or inhomogeneity of the tube morphology, there may exist strong curvature effect in experimental BNNT samples. To address this issue, we extend our investigation to the adsorption of PTD on BN tubes with different radii, where the curvature effect on the interaction between PTD and BN tubes will be discussed.

A series of zigzag tubes (n = 8, 10, 12, 15) are employed in the present work. By using the LDA calculations with BSSE correction, we examined the interaction between PTD molecule and BN tubes. After structural optimization, it is found that stacking configurations between PTD and BNNTs are similar to that of PTD−BNsheet system (displayed in Figure 4a). Following the procedure that was employed on PTD−BNsheet, the binding energy between PTD and BNNTs are simulated. Figure 4b presents our simulated binding energy curves for the adsorption of PTD on various BNNTs and BN sheet. It is clear that, as the tube radius increases, the interaction between PTD and BN systems are enhanced, with the increase of equilibrium separation distance and binding energy between PTD and BN tubes. Moreover, as the tube radius approaches to the infinity, the binding energy would approach the binding en-

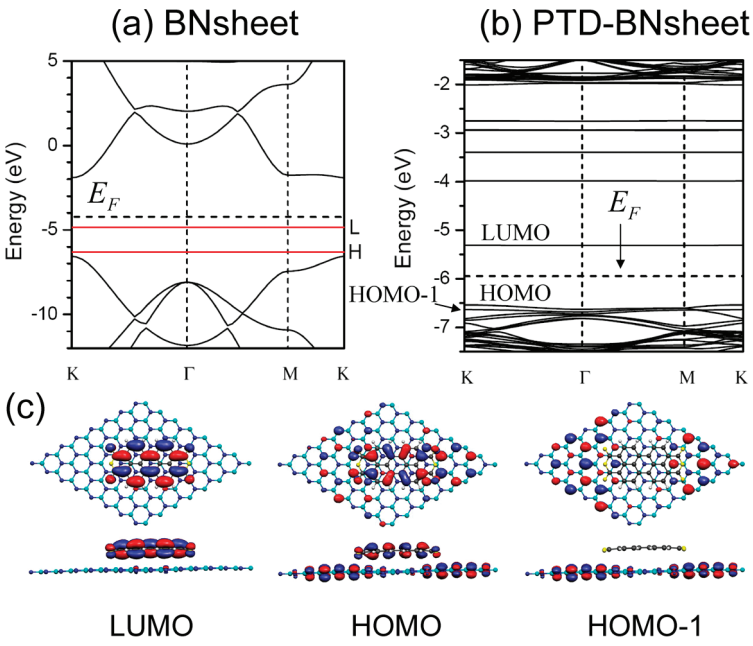

Figure 5. Band structures for (a) an isolated BN sheet and (b) the PTD−BNsheet. The LUMO and HOMO energy levels of an isolated PTD molecule are indicated by red lines (L and H) in panel a. (c) Isosurface plots of the squared wave functions at the Γ point for LUMO, HOMO, and HOMO-1 (the first energy band below HOMO) of PTD−BNsheet. The isosurface value is ±0.05 eV/Å^3 (distinguished by red and blue surface).

ergy of PTD on BNsheet. For all the BN tubes we considered, their interaction energy curve exhibits the same Lennard-Jones like characters. Our findings clearly indicate that the curvature effect of the BN tubes can only modify the intensity of their interaction between PTD molecule, while the nature of the interaction remain unchanged—it is still the van der Waals interaction. In this way, the physical properties between PTD−BNNTs and PTD−BNsheet are qualitatively the same. Therefore, in the following discussion, we will restrict our investigation to the PTD−BNsheet system only.

Red-Shift of the Adsorption Spectra. In experiments, a red-shift of the absorption band for PTAS−BNNTs relative to that of PTAS solution has been observed (Figure 2b). Such an experimental finding surprisingly suggests that the electronic properties of BNNTs can be effectively modified by the noncovalent functionalization. In our work, to reveal the effect of PTD adsorption on the electronic properties of BN system, the electronic band structure for PTD−BNsheet has been calculated and presented in Figure 5. For comparison, the band structures for an isolated BN sheet and PTD molecule are also given.

As shown in Figure 5a, an isolated BN sheet is a direct band gap semiconductor, while the HOMO and LUMO of the isolated PTD molecule are located at the band gap region of the BN sheet. The HOMO level of the isolated PTD molecule and BN sheet are discrete in energy. In particular, after the adsorption of PTD molecule on the BN sheet, the HOMO of the system falls into the valence bands, and the effective band gap of PTD−BNsheet is calculated to be 1.315 eV (at Γ point), smaller than that of the isolated PTD molecule. Although PTD molecule is adsorbed on BN sheet through the van der Waals interactions, the band structure of the entire system is not the simple superposition of energy bands of the individual PTD and BN sheet. Such a finding can lead to an important experimental consequence: the electronic properties of BNNT systems can be effectively modified through noncovalent functionalization by perylene derivative molecules.

For an adsorbate-surafce system, the nature of its electronic properties should primarily depend on the alignment of π orbitals with respect to the Fermi level.[29] Therefore, in order to deeply understand electronic properties of the PTD−BNsheet system, its energy bands around the Fermi level (shown in Figure 5c) are carefully examined. The LUMO of PTD−BNsheet corresponds to a flat energy band, which is 0.60 eV above of Fermi level. Its spatial charge distribution is almost identical to that of the isolated PTD molecule. The HOMO of PTD−BNsheet locates at the valence bands maximum (VBM), about 0.70 eV below Fermi level. Especially, the HOMO band corresponds to the π states that are both localized on PTD molecule and BN sheet. In fact, such a mixed-state character does not imply any hybridization between the orbitals from substrate and molecule, as it is in the case of a chemisorption process.[28,30] Moreover, for the energy bands below HOMO, such as HOMO-1 band shown in Figure 5c, the corresponding π states are localized at BN sheet only, but their spatial distribution are changed. Such a charge redistribution could lead to change in the dispersion of the corresponding energy bands (energy bands below VBM, Figure 5b). Consequently, the mixing state and charge redistribution characters within the PTD−BNsheet strongly demonstrate that the adsorption of PTD molecule on the BN sheet should be qualified as the physisorption. Similar electronic property features are also found in PTD-functionalized BN tubes (see the Supporting Information for a detailed analysis).

In particular, a small down shift of molecule orbitals is also observed in PTD−BNsheet, indicating there is a net transferred charge from PTD molecule within the molecule−sheet system. This finding is further confirmed by our mulliken population analysis results, that the carbon atoms will lose their π electrons after PTD is

adsorbed on BN sheet. The amount of the transferred charges are calculated to be 0.596 C (that is 0.025 C per carbon atom, by LDA calculations). Actually, the feature of orbital mixing as well as the net transferred charge are also found in other physisorbed systems, such as multiwalled CNTs[31,32] and BNNTs.[33]

In this study, the observed charge transfer could be rationalized by the charge redistribution characters within the PTD−BNsheet system. For a van der Waals interaction system, its ground state electronic charge must be redistributed to produce the required force between the adsorbate and substrate.[34] This charge redistribution can lead to the change on the physical quantities of the whole system, such as interface dipoles and work functions, *etc*.[35] In the present case, the change of the physical quantities are reflected on the net transferred charge within the PTD−BNsheet system. Compared with the chemisorbed systems, where the pronounced transferred charge is induced by strong hybridization of orbitals, the charge transfer within a physisorbed system is usually small,[34] which is ignored in most cases. However, in the present study, it is found that the charge transfer within PTD−BNsheet system is significant, which is crucial to determine the electronic properties of the perylene derivative molecules functionalized BNNTs. Typically, since the π electrons have been transferred from PTD, the energy level of the π band of PTD will go down and finally locate at the same energy range with π bands of BN sheet. In this way, compared to the isolated PTD molecule, the amount of π electrons localized at PTD within the molecule−sheet system are smaller. Therefore, the less effective coupling of the π electrons within the PTD molecule will finally lead to a smaller band gap ($\pi-\pi^*$ electronic gap) of the system.

The optical properties for PTD-functionalized BN sheet are also investigated. Figure 2a plots the simulated optical adsorption spectrum for PTD−BNsheet. The red shift of its adsorption band relative to that of PTAS solution is found in our simulation (the corresponding experimental optical peaks are indicated by arrows in Figure 2b). Although our simulations are qualitatively consistent with the experimental findings, the absolute energy is underestimated: in our simulation, the optical band is shifted by 0.147 eV, which is smaller than the experimental result 0.435 eV (~102 nm).[16] As discussed above, LDA calculations could only be used as the reasonable approximation to describe the van der Waals interactions. To precisely predict the physical properties of PTD−BNsheet system, one needs to employ more accurate van der Waals (vdW) density functional.[23] It is expected that the interaction energy between PTD and BN sheet predicted by this functional will be stronger, and the system may characterize a smaller molecule−sheet separation.[29] The larger interaction energy and smaller separation will probably lead to more mixing orbitals and transferred charge between PTD and BN sheet. Consequently, within the vdW functional calculations, the corresponding optical band should be red-shifted by a larger energy, which will be much closer to experimental results. Even so, the underlying physics revealed by LDA calculations for the perylene derivative molecules functionalized BNNTs proposed in this work should not be changed. Therefore, our calculations can still provide reasonable theoretical support to experiments.

CONCLUSIONS

First-principles calculations have been performed to study the structural and electronic properties for the perylene derivative molecules functionalized BNNTs. Two kinds of perylene derivative molecules, namely PTD and PTAS−K molecules are considered in our calculations. By simulating the adsorption of the PTD molecule on the hexagonal BN sheet and BN tubes, it is suggested that the experimental noncovalent functionalization of BNNTs with PTAS molecules is achieved through the van der Waals interactions between the adsorbate and BN substrate. In particular, our calculations indicate that the physical adsorption of the PTD molecule on the BN sheet can modify the electronic states around the Fermi level. Furthermore, it is illustrated that the net transferred charge within the PTD−BNsheet system could provide the explanation to the experimentally observed red-shift of the optical adsorption bands. Our simulations show qualitatively the same trend with the experimental measurements. Further theoretical studies on the perylene derivative molecules functionalized BNNTs using the more accurate van der Waals functionals are awaited to confirm our results.

COMPUTATIONAL MODELS AND METHODS

Our first principle calculations are preformed using SIESTA code,[36−38] which implements a density functional method by means of a numerical linear combination of an atomic-like orbital basis set.[39] The electron exchange-correlation potential is treated within the local density approximation (LDA), with Perdew and Zunger parametrization.[40] For a cross check, we also carry out our calculations with GGA in the form of PBE.[41] Standard norm-conserving Troullier−Martins pseudopotentials[42] are used to describe the interaction between ionic cores and localized pseudoatomic orbitals. Split-valence double-ζ plus polarization basis (DZP) ensures a good computational convergence with respect to the basis set. The real-space integration is performed on a regular grid corresponding to a plane-wave cutoff of 200 Ry. Mulliken population analysis is used to calculate the number of electrons occupied on each atomic orbitals.

To simulate the interaction between PTD and BNsheet, a $8 \times 8 \times 1$ BN sheet supercell, with a vacuum of 20 Å along the *z* direction is employed. Such a supercell is large enough to ensure negligible interactions between the periodic images. The Brillouin zone

is sampled using the Monkhorst−Pack special *k*-point scheme[43] with a 8 × 8 × 1 mesh for structural optimization and total energy calculations. For PTD−BNtube systems, the zigzag BN tubes, which consist of five times of primary unit cell along the axial direction are employed in our calculation. Periodical boundary condition is imposed along the axial direction of BNNT, and a vacuum region (at least 20 Å is assumed between the tubes in their lateral direction. A set of six Monkhorst−Pack special *k* points along the tube axis is used. The conjugate gradient (CG) algorithm is adopted to fully relax the structures until the residual force acting on each atom is no more than 0.02 eV/ Å.

Acknowledgment. G. Y. Gou thanks Weitai Wu and Seungchul Kim for their useful discussions. Doyle Yuan is acknowledged for his revision of the manuscript. This work is financially supported by National Basic Research Program of China (2009CB939900), National Science Foundation of China (Grant No. 10874161) and the Innovation Foundation of USTC for the Postgraduate (KD2007079). The HP-LHPC of USTC is acknowledged for computational support.

Supporting Information Available: Energy band diagram and isosurface charge density of the PTD-functionalized (10, 0) BN tube. This material is available free of charge *via* the Internet at http://pubs.acs.org.

REFERENCES AND NOTES

1. Rubio, A.; Corkill, J. L.; Cohen, M. L. Theory of Graphitic Boron Nitride Nanotubes. *Phys. Rev. B* **1994**, *49*, 5081–5084.
2. Chopra, N. G.; Luyken, R. J.; Cherrey, K.; Crespi, V. H.; Cohen, M. L.; Louie, S. G.; Zettl, A. Boron−Nitride Nanotubes. *Science* **1995**, *269*, 966–967.
3. Blase, X.; Rubio, A.; Louie, S. G.; Cohen, M. L. Stability and Band-Gap Constancy of Boron−Nitride Nanotubes. *Europhys. Lett.* **1994**, *28*, 335–340.
4. Chen, Y.; Zhou, J.; Campell, S. J.; Le Caer, G. Boron Nitride Nanotubes: Pronounced Resistance to Oxidation. *Appl. Phys. Lett.* **2004**, *84*, 2430–2432.
5. Chang, C. W.; Fennimore, A. M.; Afanasiev, A.; Okawa, D.; Ikuno, T.; Garcia, H.; Li, D. Y.; Majumdar, A.; Zettl, A. Isotope Effect on the Thermal Conductivity of Boron Nitride Nanotubes. *Phys. Rev. Lett.* **2006**, *97*, 085901−1085901−4.
6. Hernández, E.; Goze, C.; Bernier, P.; Rubio, A. Elastic Properties of C and $B_xC_yN_z$ Composite Nanotubes. *Phys. Rev. Lett.* **1998**, *80*, 4502–4505.
7. Suryavanshi, A. P.; Yu, M.; Wen, J.; Tang, C. C.; Bando, Y. Elastic Modulus and Resonance Behavior of Boron Nitride Nanotubes. *Appl. Lett. Phys.* **2004**, *84*, 2527–2529.
8. Zhi, C. Y.; Bando, Y.; Tang, C. C.; Huang, Q.; Golberg, D. Boron Nitride Nanotubes: Functionalization and Composites. *J. Mater. Chem.* **2008**, *18*, 3900–3908.
9. Tang, C. C.; Bando, Y.; Huang, Y.; Yue, S. L.; Gu, C. Z. Fluorination and Electrical Conductivity of BN Nanotubes. *J. Am. Chem. Soc.* **2007**, *127*, 6552–6553.
10. Zhi, C. Y.; Bando, Y.; Tang, C. C.; Golberg, D. Engineering of Electronic Structure of Boron−Nitride Nanotubes by Covalent Functionalization. *Phys. Rev. B* **2006**, *74*, 153413−1153413−4.
11. Gou, G. Y.; Pan, B. C.; Shi, L. Interaction of Iron Atoms with Pristine and Defective (8, 0) Boron Nitride Nanotubes. *J. Phys. Chem. C* **2008**, *112*, 13571–13578.
12. Chen, Z. G.; Zou, J.; Li, F.; Liu, G.; Tang, D. M.; Li, D.; Liu, C.; Ma, X. L.; Cheng, H. M.; Lu, G. Q.; *et al.* Growth of Magnetic Yard-Glass Shaped Boron Nitride Nanotubes with Periodic Iron Nanoparticles. *Adv. Funct. Mater.* **2007**, *17*, 3371–3377.
13. Zhi, C. Y.; Bando, Y.; Tang, C. C.; Honda, S.; Sato, K.; Kuwahara, H.; Golberg, D. Covalent Functionalization: Towards Soluble Multiwalled Boron Nitride Nanotubes. *Angew. Chem.* **2005**, *117*, 8146–8149.
14. Wu, X. J.; An, W.; Zeng, X. C. Chemical Functionalization of Boron−Nitride Nanotubes with NH_3 and Amino Functional Groups. *J. Am. Chem. Soc.* **2006**, *128*, 12001–12006.
15. Zhi, C. Y.; Bando, Y.; Tang, C. C.; Xie, R. G.; Sekiguchi, T.; Golberg, D. Perfectly Dissolved Boron Nitride Nanotubes Due to Polymer Wrapping. *J. Am. Chem. Soc.* **2005**, *127*, 15996–15997.
16. Wang, W. L.; Bando, Y.; Zhi, C. Y.; Fu, W. Y.; Wang, E. G.; Golberg, D. Aqueous Noncovalent Functionalization and Controlled Near-Surface Carbon Doping of Multiwalled Boron Nitride Nanotubes. *J. Am. Chem. Soc.* **2008**, *130*, 8144–8145.
17. Huang, Q.; Sandanayaka, A.; Bando, Y.; Zhi, C. Y.; Ma, R. Z.; Shen, G. Z.; Golberg, D.; Zhao, J. C.; Araki, Y.; Ito, O.; *et al.* Donor−Acceptor Nanoensembles Based on Boron Nitride Nanotubes. *Adv. Mater.* **2007**, *19*, 934–938.
18. Zhi, C. Y.; Bando, Y.; Tang, C. C.; Honda, S.; Sato, K.; Kuwahara, H.; Golberg, D. Characteristics of Boron Nitride Nanotube−Polyaniline Composites. *Angew. Chem., Int. Ed.* **2005**, *44*, 7929–7932.
19. Gou, G. Y.; Pan, B. C.; Shi, L. The Nature of Radiative Transitions in O-Doped Boron Nitride Nanotubes. *J. Am. Chem. Soc.* **2009**, *131*, 4839–4845.
20. Hybertsen, H. S.; Louie, S. G. First-Principles Theory of Quasiparticles: Calculation of Band Gaps in Semiconductors and Isulators. *Phys. Rev. Lett.* **1985**, *55*, 1418–1421.
21. Hybertsen, H. S.; Louie, S. G. Electron Correlation in Semiconductors and Insulators: Band Gaps and Quasiparticle Energies. *Phys. Rev. B* **1986**, *34*, 5390–5413.
22. Lima, M. P.; Fazzio, A.; da Silva, A. J. R. Edge Effects in Bilayer Graphene Nanoribbons: *Ab Initio* Total-Energy Density Functional Theory Calculations. *Phys. Rev. B* **2009**, *79*, 153401-1–153401-4.
23. Dion, M.; Rydberg, H.; Schröder, E.; Langreth, D. C.; Lundqvist, B. I. Van der Waals Density Functional for General Geometries. *Phys. Rev. Lett.* **2004**, *92*, 246401-1–246401-4.
24. Tournus, F.; Charlier, J.-C. *Ab initio* Study of Benzene Adsorption on Carbon Nanotubes. *Phys. Rev. B* **2005**, *71*, 265421−1265421−8.
25. Boys, S. F.; Bernardi, F. The Calculation of Small Molecular Interactions by the Differences of Separate Total Energies. Some Procedures with Reduced Errors. *Mol. Phys.* **1970**, *19*, 553–566.
26. Hasegawa, M.; Nishidate, K.; Iyetomi, H. Energetics of Interlayer Binding in Graphite: The Semiempirical Approach Revisited. *Phys. Rev. B* **2007**, *76*, 115424-1–115424-8.
27. Henwood, D.; Carey, J. D. *Ab Initio* Investigation of Molecular Hydrogen Physisorption on Graphene and Carbon Nanotubes. *Phys. Rev. B* **2007**, *75*, 245413-1–245413-10.
28. Tournus, F.; Latil, S.; Heggie, M. I.; Charlier, J.-C. π-Stacking Interaction between Carbon Nanotubes and Organic Molecules. *Phys. Rev. B* **2005**, *72*, 075431-1–075431-5.
29. Atodiresei, N.; Caciuc, V.; Lazić, P.; Blügel, S. Chemical *versus* van der Waals Interaction: The Role of the Heteroatom in the Flat Absorption of Aromatic Molecules C_6H_6, C_5NH_5, and $C_4N_2H_4$ on the Cu(110) Surface. *Phys. Rev. Lett.* **2009**, *102*, 136809-1–136809-4.
30. Giannozzi, P. Comment on "Noncovalent Functionalization of Carbon Nanotubes by Aromatic Organic Molecules" [*Appl. Phys. Lett.* **2003**, *82*, 3746]. *Appl. Phys. Lett.* **2004**, *84*, 3936–3938.
31. Miyamoto, Y.; Saito, S.; Tománek, D. Electronic Interwall Interactions and Charge Redistribution in Multiwall Nanotubes. *Phys. Rev. B* **2001**, *65*, 041402-1–041402-4.
32. Zólyomi, V.; Koltai, J.; Rusznyák, Á.; Kürti, J.; Gali, Á.; Simon, F.; Kuzmany, H.; Szabados, Á.; Surján, P. R. Intershell Interaction in Double Walled Carbon Nanotubes: Charge Transfer and Orbital Mixing. *Phys. Rev. B* **2008**, *77*, 245403−1245403−10.
33. Okada, S.; Saito, S.; Oshiyama, A. Interwall Interaction and Electronic Structure of Double-Walled BN Nanotubes. *Phys. Rev. B* **2002**, *65*, 165410−1165410−4.

34. Thonhauser, T.; Cooper, V. R.; Li, S.; Puzder, A.; Hyldgaard, P.; Langreth, D. C. Van der Waals Density Functional: Self-Consistent Potential and the Nature of the van der Waals Bond. *Phys. Rev. B* **2007**, *76*, 125112−1125112−11.
35. Bagus, P. S.; Hermann, K.; Wöll, C. The Interaction of C_6H_6 and C_6H_{12} with Noble Metal Surfaces: Electronic Level Alignment and the Origin of the Interface Dipole. *J. Chem. Phys.* **2005**, *123*, 184109−1184109−13.
36. Ordejón, P.; Artacho, E.; Soler, J. M. Self-Consistent Order-N Density-Functional Calculations for Very Large Systems. *Phys. Rev. B* **1996**, *53*, R10441–10444.
37. Sánchez-Portal, D.; Ordejón, P.; Artacho, E.; Soler, J. M. Density-Functional Method for Very Large Systems with LCAO Basis Sets. *Int. J. Quantum Chem.* **1997**, *65*, 453–461.
38. Soler, J. M.; Artacho, E.; Gale, J. D.; García, A.; Junquera, J.; Ordejón, P.; Sánchez-Portal, D. The SIESTA Method for *ab Initio* Order-N Materials Simulation. *J. Phys.: Condens. Matter* **2002**, *14*, 2745–2779.
39. Sankey, O. F.; Niklewski, D. J. *Ab Initio* Multicenter Tight-Binding Model for Molecular-Dynamics Simulations and Other Applications in Covalent Systems. *Phys. Rev. B* **1989**, *40*, 3979–3995.
40. Perdew, J. P.; Zunger, A. Self-Interaction Correction to Density-Functional Approximations for Many-Electron Systems. *Phys. Rev. B* **1981**, *23*, 5048–5079.
41. Perdew, J. P.; Burke, K.; Ernzerhof, M. Generalized Gradient Approximation Made Simple. *Phys. Rev. Lett.* **1996**, *77*, 3865–3868.
42. Troullier, N.; Martins, J. L. Efficient Pseudopotentials for Plane-Wave Calculations. *Phys. Rev. B* **1991**, *43*, 1993–2006.
43. Monkhorst, H. J.; Pack, J. D. Special Points for Brillouin-Zone Interactions. *Phys. Rev. B* **1976**, *13*, 5188–5192.